Electron Energy Distributions from Ionizing Collisions of Helium and Neon Ions with Helium*

R. B. BARKER† AND H. W. BERRY
Department of Physics, Syracuse University, Syracuse, New York
(Received 22 June 1966)

The electron-energy distributions arising from ionizing collisions of He and Ne ions with a He target have been examined under conditions such that the instrumental resolutions does not affect the distribution. Incident ions were in the range of 1–4 keV. The distributions consist of a sharp maximum near the zero of the electron energy with broader peaks occurring in the 20–40-eV region. Two broad peaks are detectable in the He^+-He spectrum and six are found in the Ne^+-He spectrum. The energy of the maxima of the prominent broad peaks have been found to fit a linear dependence on the inverse ion velocity over all or part of the ion range investigated. This dependence, when extrapolated to infinite ion energy, has yielded peak energies which correspond to previously identified auto-ionizing states. Where measurement is possible, these same peaks show a decrease in width at half-maximum also linear with the inverse ion velocity. A model is presented which attributes the observed behavior to a collision-induced excitation of auto-ionizing states followed by autoionization transitions which occur in the field of the ion.

INTRODUCTION

A SERIES of studies[1] of the energy distribution of electrons from ionizing collisions of various combinations of rare gas ions and atoms of about 1-keV energy has shown that at least a part of the ionization occurs through the Auger process of auto-ionization. The auto-ionization electrons appear in the spectrum as broad peaks which are superimposed on a continuous distribution that generally decreases with increasing electron energy and ends in one of the auto-ionization peaks. The interpretation of these peaks as representing auto-ionization electrons has been substantiated by experiments on far ultraviolet absorption,[2] electron scattering,[3] and ionization of the rare gases by fast protons and H_2^+ ions,[4] as well as by theoretical calculations of the energy of the auto-ionizing states of the He atom.[5] The ultraviolet-absorption studies and the theoretical calculation, in particular, indicate that the energy width of the auto-ionizing state is small, less than 0.1 eV. This is in contrast to the width of several eV of the peaks observed in these studies of slow collisions of He ions and atoms.

There exists also a disturbing difference between the auto-ionizations by fast protons in He and that produced by slow collisions of He^+ ions in He. For fast protons, Rudd[4] has found at least seven peaks, and the theoretical calculations predict more than ten auto-ionizing states in He for which the energy of the ejected electron will be in the range of 30 to 40 eV. The measurements for slow He^+ ions in He, however, show only one pronounced auto-ionization peak with just a suggestion of one several eV higher. There should be, though, ample energy to excite many of the other auto-ionizing states at the highest ion energy used, 4.3 keV.

In the experiment reported here, the electron spectra from ionizing collisions of He^+ in He have been re-examined under conditions such that the instrumental resolution does not materially affect the observed linewidth. This has not produced, though, any sizeable change in the width of the auto-ionization peak in He. However, for the electron spectra for Ne^+ in He, the improved resolution did bring out more detail in the distribution than was previously reported.[1] This earlier study found that the auto-ionization peaks showed a definite shift with ion velocity. Such a shift has now been found for He^+ in He.

A discussion of the general experimental method, the observed energy distributions, and the interpretation of these in terms of the states of the temporary molecule formed in the collision follow.

EXPERIMENTAL METHOD

The procedure consists first in producing an e/m analyzed ion beam with an energy of the order of 1 keV. This beam can be further accelerated and neutralized, if desired, before entering the ionization chamber where the target gas is contained. An aperture in this chamber allows electrons ejected at 90° with the beam in the collision to enter an energy analyzer. Electrons falling within a specific energy interval then enter a secondary electron multiplier with the output of this fed into an amplifier and a chart recorder.

* This work was supported in part by the National Science Foundation.

† Present address: Lawrence Radiation Laboratory, University of California, Livermore, California.

[1] H. W. Berry, Aeronautical Research Laboratory (Wright–Patterson Air Force Base) Report 185, 1961 (unpublished); Phys. Rev. **121**, 1714 (1961); **127**, 1634 (1962).

[2] R. P. Madden and K. Codling, Phys. Rev. Letters **10**, 516 (1963); **12**, 106 (1964); Astrophys. J. **141**, 364 (1965); J. Opt. Soc. Am. **54**, 268 (1964).

[3] J. Arol Simpson, S. R. Mielczarek, and J. Cooper, J. Opt. Soc. Am. **54**, 269 (1964).

[4] M. E. Rudd, Phys. Rev. Letters, **13**, 503 (1964); **15**, 580 (1965).

[5] F. G. Fender and J. P. Vinti, Phys. Rev. **46**, 77 (1934); Ta-You Wu, *ibid.* **46**, 239 (1934); **66**, 291 (1944); W. M. Cady, *ibid.* **46**, 439 (1934); W. Wilson, *ibid.* **48**, 536 (1935); B. H. Bransden and A. Dalgarno, Proc. Phys. Soc. (London) **A66**, 904 (1953); R. K. Propin, Opt. Spectr. USSR **8**, 159 (1960); J. W. Cooper, *Atomic Collision Processes* (North-Holland Publishing Company, Amsterdam, 1964), p. 607; P. G. Burke, D. D. McVicar, and K. Smith, Phys. Rev. Letters **11**, 559 (1963); Proc. Phys. Soc. (London) **83**, 397 (1964); **84**, 749 (1964); **86**, 989 (1965).

The ionization chamber is a gold-plated cylinder with an internal diameter of 0.875 in. and a length of 2.25 in. The ends are covered with diaphragms and annular rings for defining the beam and quenching the secondary electron emission from the aperture edges. Within the cylinder and concentric with it is a grid composed of 24 one-mil tungsten wires spaced at 15° intervals and placed parallel to the beam direction. The grid is wound from a continuous tungsten wire through properly located holes in an insulator at the cylinder ends. The electron energy analyzer is a 90° electrostatic type composed of gold-plated cylindrical quadrants. The entrance and exit apertures are slits 20 mils wide. For such an analyzer the energy spread is a fixed percentage of the energy passed and for this analyzer it has the ideal value of 1.33×10^{-2}.

Since the analyzer has zero width for zero-energy electrons, it is necessary that some energy be added to all electrons coming from the collision process, if the electron spectrum is to extend with any accuracy to those electrons with energies near zero. This energy is provided by potential differences between the grid and the ionization chamber and between the chamber and the entrance to the analyzer. To determine the optimum ratio of these potential differences so that the low-energy yield would not be distorted, an electrolytic tank study and a computer analysis of the potential within the grid and between the grid and the ionization chamber on the exit slit side were made. The result of this study which is of major interest here concerns the potential in the space within the grid. It was found that in the volume whose radius is 0.72 of the radius on which the grid wires lie, the potential is constant to five significant figures and has a value of 0.8125 of the potential difference between the grid wires and the ionization chamber. Since the beam diameter is about one-tenth of this, the electrons from ionizing collisions are generated in a field-free region. A variation of the division of these potential differences, but keeping the total constant, allows that part of the electron spectrum arising from ionizing collisions to shift in absolute energy though leaving the contribution of the secondary emission from the grid wires and the edges of the exit slit fixed. In this way any ambiguity of origin of a specific structure in the electron spectrum can be resolved.

In continuous recording of the data as was done here, the time constant of the measuring circuit will, if the recording is done too rapidly, produce an apparent shift in the position of a sharp peak. This was especially evident in the zero-energy peak, which has a sharp rise on one side followed by a slower decline on the other. See Fig. 1. The effect of the response time could be observed by sweeping the spectrum in both directions. An adjustment of the sweep rate and the circuit time constant was always made, so that there was no measurable difference in the spectrum taken with increasing or with decreasing electron energy.

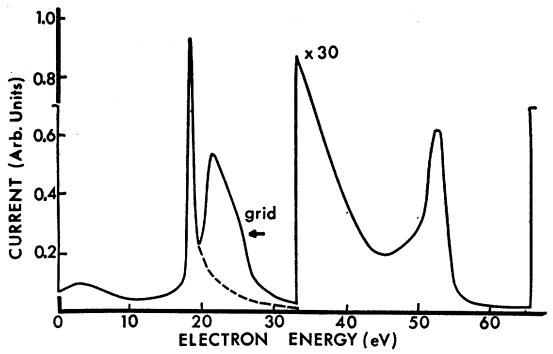

FIG. 1. A representative electron-energy distribution for 1.8-keV He^+ in He. The ordinate is the electron yield per eV range in arbitrary units. The abscissa is the energy of the electron after acceleration. The sharp peak at about 18 eV occurs at an energy which corresponds to electrons of zero self-energy. The peak marked "grid" should be ignored since this represents the current from the grid produced by the neutralization of the He^+ ion on the grid wires.

EXPERIMENTAL RESULTS

Figure 1 shows a drawing of the electron spectrum for a 1.8-keV He^+ in He. The curve represents an average of several actual data records thus eliminating the effects of noise. The two salient features of the spectrum are the sharp peak at 18.4 eV and the broad peak at 53 eV. The first called the "zero peak" occurs at an energy within a few tenths of an eV of the energy expected for an electron that originates in the center of the grid with essentially zero kinetic energy. The peak marked "grid" represents electrons ejected from the grid wires by ion bombardment. These secondary electrons can always be distinguished from the ionization electrons by a variation of the potential difference ratio of the electron accelerating voltages as described above.

The energy at which electrons of zero self-energy would be recorded is not sufficiently well known from the applied potential difference because of the penetration of the field into the region within the grid and of the existence of contact potential differences. Evidence also occasionally appeared that indicated a surface charge on the grid that caused a shift in the absolute position of the spectrum with time. Cleaning of the grid always restored the spectrum to its initial position. To determine unequivocally the absolute energy of the zero peak, a series of data runs were made in which first the grid voltage was varied, and then a series in which the grid voltage was held constant but the potential difference between the ionization chamber and the analyzer was varied. A plot of the position of the zero-energy peak against the grid voltage yielded a straight line with a slope of 0.81 ± 0.01 which is in excellent agreement with the calculated value of 0.8125. For the second set, a plot of the position of the zero peak as a function of the applied potential difference gave the calibration constant of the analyzer. This again is in good agreement with the value calculated from the

geometry of the analyzer. This constant was checked frequently during the course of recording the data.

A critical factor in the interpretation of the spectrum is the effect of the instrumental resolution on the shape of the peaks. Coupled with the fact that electrons from the ionizing collisions can not be expected to have less than zero kinetic energy, the sharp rise of the zero peak is suggestive of the possibility that the finite energy width of the analyzer plays a strong role here. This is particularly evident if one examines the rise time on the low-energy side of the zero peak as the zero peak is shifted to higher energy by increasing the electron accelerating potential difference. The rise time was found to increase linearly with the zero-peak energy in accord with the behavior of the resolution of this kind of analyzer. Since the resolution is dependent on the accuracy of alignment, these measurements were repeated frequently with an average slope of 2% and a deviation of 0.3%.

If one assumes that an ideal distribution of the type observed here would have an infinitely fast rise to a maximum followed by something like an exponential drop, then the effect of a finite slit width is readily computed. The calculation indicates that the onset of the distribution will have a rise time equal to the energy width accepted by the analyzer, and the half-maximum height will occur at the energy corresponding to that of the infinitely fast rise. This center of the rise was chosen as the zero of the electron energy. It is felt that this is valid to within ± 0.1 eV.

The Electron Energy Distribution for He^+ in He

Representative curves of the auto-ionization peak for ionizing collisions of He^+ in He are shown in Fig. 2. As is done in Fig. 1, these are drawn relative to the zero peak height, and for comparison here an arbitrary ordinate unit is used such that the 4.3-keV curve has unit height. As mentioned above, not only does the energy at which the auto-ionization peak occurs shift to higher energy but also there occurs a decrease in width at half-maximum of the peak with increasing ion velocity. An analysis has shown the peak energy to have a linear dependence on the inverse square root of the ion energy for the range measured of about 1.2- to 4.3-keV ion energy. Since the data obtained in a single run are generally of higher self-consistency than data for runs at different times, a single set is fitted to the best straight line by a least-squares analysis. For many similar data sets, an average formula for the straight line expressing the auto-ionization peak energy as a function of the ion energy V in keV is $(35.78\pm0.23) - (37.9\pm9.7)V^{-1/2}$ eV. Assuming the validity of the extrapolation, the peak at infinite ion energy would, therefore, occur at (35.78 ± 0.23) eV.

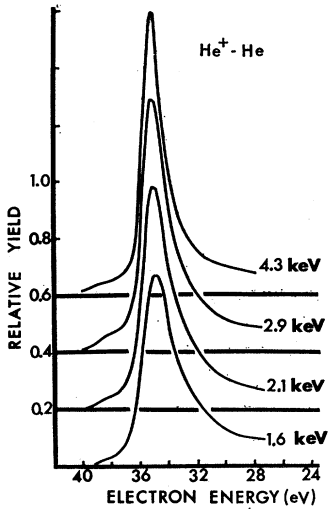

FIG. 2. The electron-energy distribution for the auto-ionization peak for collisions of He^+ in He for four different ion energies.

A similar analysis was made of the width at half-maximum. This also shows a linear behavior with the inverse square root of the ion energy. An average of several least-squares analyses of individual data sets gave for the peak width at half-height $(0.41\pm0.25) + (94.4\pm7.0)V^{-1/2}$ eV. If the width continues to decrease with increasing ion energy in the manner indicated, the experimentally observed width will be limited by the energy width of the analyzer. The width value obtained from the above relationship for infinite ion energy is consistent with the analyzer width.

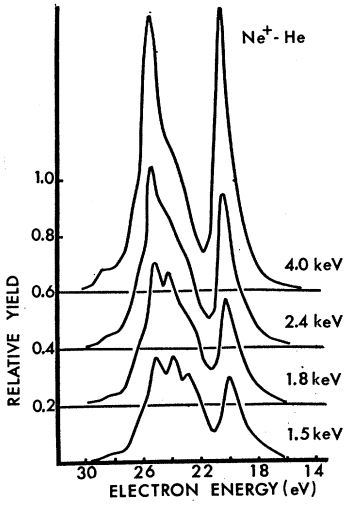

FIG. 3. The electron-energy distribution for the auto-ionization peaks for collisions of Ne^+ in Ne for four different ion energies.

In obtaining the measurements used for the analysis of the peak energy shift with ion energy, a grid voltage of 28 V relative to the analyzer entrance was used. This had the effect of shifting the secondary electron grid peak away from the zero peak, so that the separation of the zero peak and the auto-ionization peak could be accurately measured. The long high-energy tail of the grid contribution did project into the region of the auto-ionization peak but not significantly enough to distort the peak location. For the data used to determine the width, however, a grid voltage of 14 V was used. This resulted in severe distortion of the zero peak, which was not of interest here, but also produced a shift of the

entire spectrum to lower energies thus effectively increasing the resolution and so the accuracy of the width measurement. The dependence of the auto-ionization peak width on ion beam velocity was also examined for the case where the grid was at 28 V relative to the analyzer. For this, an estimated grid secondary-electron contribution was subtracted from the low-energy side of the auto-ionization peak. The relationship here was found to be $(1.50\pm0.20)+(89.2\pm8.0)V^{-1/2}$ eV. This is in good agreement with that found for the lower grid voltage, and the intercept is about that expected for the larger analyzer width caused by the peak falling at a higher total energy. The data curves in Fig. 2 suggest a peak at 38.5 eV. This was not of sufficient size to analyze in the same way as was done for the 36-eV peak.

TABLE I. Comparison of He auto-ionizing state energies with electron ejection energies from ionizing collisions.

Ejection energies (eV) Present results	Rudd[a]	Auto-ionization energies (eV) Simpson *et al.*[b]	Madden and Codling[c]	Theory: Burke, *et al.*[d]	He state identification[e]
	33.24(57.82)[f]	57.9		57.87	$(2s)^2\,{}^1S$
	33.76(58.34)	58.5		58.36	$(2s)(2p)\,{}^3P$
	35.42(60.0)	60.0			$(2p)^2\,{}^1D$
35.8(60.4)[f]	35.52(60.1)	60.1	60.12	60.27	$(sp, 22-)\,{}^1P$
	37.57(62.15)				$(2p)^2\,{}^1P$
	38.20(62.78)		62.76	62.77	$(sp, 23-)\,{}^1P$
	38.37(62.95)			63.01	$(2s)(3s)\,{}^1S$
	38.50(63.08)			63.14	$(2s)(3p)\,{}^3P$
	39.07(63.65)	63.6	63.65	63.69	$(sp, 23+)\,{}^1P$
39.5?(64.1)			64.14	64.13	$(sp, 24-)\,{}^1P$
	39.64(64.22)			64.22	$(2s)(4s)\,{}^1S$
		64.5	64.46	64.48	$(sp, 24+)\,{}^1P$
			64.66	64.69	$(sp, 25-)\,{}^1P$
	40.13(64.71)			64.71	$(2s)(5p)\,{}^3P$
			64.81		$(sp, 25+)\,{}^1P$

[a] Reference 4.
[b] Reference 3.
[c] Reference 2.
[d] Reference 5.
[e] See Fano and Fano *et al.* (Ref. 12) for an explanation of the notation used for the He state identification.
[f] Figures in parenthesis are corresponding state energies assuming the ion ground state as the auto-ionization transition final state.

The Electron Energy Distribution for Ne^+ in He

The electron energy distributions for ionizing collisions of Ne^+ in He have also been remeasured with the improved analyzer resolution. The earlier measurements showed only two peaks associated with the auto-ionization process. These have now been resolved into six peaks and this part of the spectrum is shown in Fig. 3. Only the two most prominent peaks, viz. at 20.7 and 25.6 eV for a 4-keV ion energy, have been examined for an energy dependence on ion velocity. Neither peak exhibits a linear dependence for the entire range examined. But for the higher ion velocities, the linearity was sufficiently good so that a least-squares analysis was possible with the result that these peak energies can be expressed as $(21.78\pm0.27)-(66\pm23)V^{-1/2}$ eV and $(26.70\pm0.29)-(69\pm18)V^{-1/2}$ eV. The 22-eV peak is the only one sufficiently well removed from the neighboring peaks for a width analysis to be made. The width at half-height is again a linear function of the inverse square root of the ion energy with the dependence given by $(0.49\pm0.20)+(37\pm10)V^{-1/2}$ eV.

TABLE II. Comparison of Ne auto-ionization state energies with electron ejection energies from ionizing collisions.

Ejection energies (eV) Present results	Rudd[a]	Auto-ionization energies (eV) Simpson *et al.*[b] I[c]	II[d]	Ne state identification[e]
	15.4(37.0)[e]			
	19.0(40.6)			
	20.4(42.0)			
21.8(43.4)[e]	21.7(43.3)			$(2s)(2p)^6(3s)\,{}^1S$
	22.2(43.8)	43.6		
		45.0	44.9	
	23.7(45.3)	45.6	45.6	$(2s)(2p)^6(3p)\,{}^1P$
24.6(46.2)	24.7(46.3)	46.5		$(2s)(2p)^6(4s)\,{}^1S$
	25.2(46.8)	47.1	47.1	$(2s)(2p)^6(4p)\,{}^1P$
	25.3(46.9)			$(2s)(2p)^6(5s)\,{}^1S$
25.6(47.2)	25.8(47.4)	47.7	47.7	$(2s)(2p)^6(5p)\,{}^1P$
26.7(48.3)	26.7(48.3)			
27.8(49.2)				
30.0(51.6)				

[a] Reference 4.
[b] Reference 3.
[c] Energies obtained from electron beam attenuation methods.
[d] Estimated by Simpson *et al.* from published ultraviolet absorption spectra of Madden and Codling (Ref. 2).
[e] Figures in parenthesis are corresponding state energies assuming the ion ground state as the auto-ionization transition final state.

INTERPRETATIONS OF RESULTS

The close agreement between most of the peak energies which are observed here and those which also have been calculated or observed under entirely different excitation mechanisms leaves little doubt that these peaks represent electrons from an auto-ionization process. See Tables I and II. Observations, however, of the width of the auto-ionization states from the ultraviolet absorption linewidth and from theoretical calculations indicate a value several orders of magnitude smaller than that observed here. Also, there is no mechanism inherent in the auto-ionization process which would account for the shift in the peak energy with ion velocity for the low velocities used. It is, therefore, suggestive that what is observed is not a simple auto-ionization of an isolated atom. The excited state is created in the field of an ion, and, because of the relatively slow ion velocity and of the short auto-ionization lifetimes, the transition occurs under conditions such that the state energies differ from those which an isolated atom would have.

Fano and Lichten,[6] in an analysis of the results of Everhart and co-workers,[7] have proposed in the case of multiple ionization by high-velocity ions that the primary source of energy dissipation stems from the electron-promotion mechanism inherent in the molecular-orbital model of the temporary molecule formed in the collision. This is then followed by an auto-ionization, if the state overlaps the continuum. A qualitatively similar argument can be applied to the ionization

[6] U. Fano and W. Lichten, Phys. Rev. Letters **14**, 627 (1956).
[7] E. Everhart and Q. C. Kissel, Phys. Rev. Letters **14**, 247 (1965).

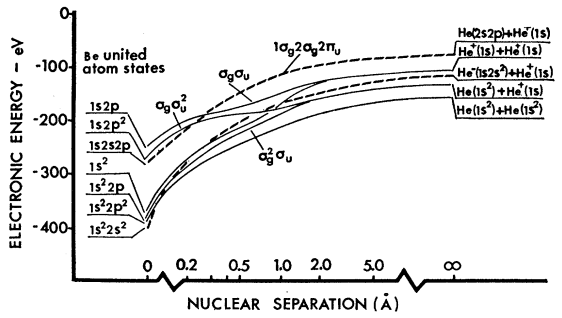

FIG. 4. The electronic energy of various He_2 molecule and molecular ion states. With the exception of $He(2s2p)=He^+(1s)$ and $He^-(1s2s^2)+He^+(1s)$ states, the curves are adapted from Lichten (Ref. 8). The curves represent the general behavior that one might expect for collisions of He^+ and He^0 on He and indicate roughly the crossings at which transitions from one state to another might occur. The zero of energy is that of the bare nuclei $He^{++}+He^{++}$.

process here by making use of diabatic molecular orbital approximation as developed by Lichten[8] from the calculations of Phillipson[9] for the case of the He_2 system. Figure 4, taken largely from Lichten, shows a number of diabatic electronic energy curves suitable for the discussion of fast collisions involving He ions and neutral atoms. The curves for $He(2s2p)+He^+(1s)$ and $He^-(1s2s^2)+He^+(1s)$ have been added. With the exception of these, which are represented by dashed lines, the curves are based on an independent particle model for which stationary molecular states are constructed from products of one electron orbital wave function. At near zero nuclear separation, the molecular orbitals go over to the atomic orbitals of the atom formed by the fusion of the He nuclei, i.e., Be. At very large nuclear separation, the molecular wave functions are expressed in terms of the wave functions of the separated atoms. For intermediate separations, linear combinations of the atomic orbitals describe the molecular orbitals. The dashed curves, however, are estimated with only the end points definitely known. This is also true for the rest of the curves for separations of less than 0.5 Å. As noted by Lichten, there is in this diabatic approximation some arbitrariness in the correspondence of the isolated atom states and those of the united atom.

An ionizing collision of a He^+ ion and a He atom could possibly be described in terms of the curves of Fig. 4 as follows: Assuming the He^+ to be in the ground state, the electronic energy of the molecule formed in the collision would be represented by the curve labeled $He(1s^2)+He^+(1s)$. If also at small internuclear separation the state is that represented by the branch $(\sigma_g\sigma_u^2)$, then at the crossing or near crossing of this curve with that of the system $He(2s2p)+He^+(1s)$ $(\sigma_g 2\sigma_g 2\pi_u)$, a transition to this state may occur. This intermediate state is an auto-ionizing state with a lifetime of the order of the collision times here. Hence, a transition is possible to the state $He^+(1s)+He^+(1s)+$free electron. The electron carries off as kinetic energy the energy difference given by the vertical separation of the two curves for the internuclear separation at which the transition occurs. At large separations, of course, the kinetic energy is equal to the energy difference between the states for the isolated atoms.

A continuous distribution of electron energies would thus be expected ranging from zero up, if the curve crossing of the intermediate and the final states occurs at greater nuclear separation than the crossing of the initial and intermediate states. For different auto-ionizing states, the distributions will depend on the lifetimes of the particular states and upon the relative velocity of the particles, provided that the initial ion energy is sufficient for the initial curve crossing to occur. For the case when the collision times are much less than the auto-ionization lifetimes, we would expect almost all of the transitions to occur when the system is describable by the individual atomic wave functions. Therefore, as with the results of Rudd,[4] the electron-energy distributions are sharply peaked at the energy expected for the isolated atom.

The importance of the molecular states is further indicated by the electron spectrum produced by ionizing collisions of He^0 with He again for a kinetic energy of several keV.[1] No peak at 35.8 eV was observed, but instead less pronounced peaks occurred at about 14 and 19 eV. Recently, a resonance in the scattering of electrons in He observed by Schultz[10] has been interpreted by Simpson and Fano[11] as the formation of the negative ion $He^-(1s2s^2)$. This could well be the origin of the 19 eV auto-ionization peak in the He^0-He collisions. The potential curves for the orbitals involved here are also shown in Fig. 4. The initial transition occurs from the state $He(1s^2)+He(1s^2)$ to $He^-(1s2s^2)+He^+(1s)$. This auto-ionizes to the state $He(1s^2)+He^+(1s)+$electron.

Neither the electronic energy or the lifetime of the states involved is sufficiently well known to calculate the electron spectrum. For large internuclear separations, however, the difference in the states $He(2s2p)+He^+(1s)$ and $He^+(1s)+He^+(1s)$ will be approximately the Coulomb potential of the ejected electron in the field of the receding ion. Also, one might expect that the lifetime of the auto-ionizing state would be nearly constant with a value about that of the auto-ionizing atom. On this basis, a simple model for the line shape of the auto-ionizing peak can be developed. The model[1] assumes also that the ion velocity is the value for infinite separation and that the internuclear distance involved is much greater than the distance of closest approach. For the case of He^+ in He, this model would indicate that the part of the distribution for an electron energy greater than 32 eV will occur for auto-ionizations at internuclear separations greater than about 5 Å. This outer end of

[8] W. Lichten, Phys. Rev. **131**, 229 (1963).
[9] P. E. Phillipson, Phys. Rev. **125**, 1981 (1962).
[10] G. J. Schultz, Phys. Rev. **136**, A650 (1964).
[11] J. A. Simpson and U. Fano, Phys. Rev. Letters, **11**, 158 (1963).
[12] U. Fano, Phys. Rev. **124**, 1866 (1961); J. Cooper, U. Fano, and F. Prats, Phys. Rev. Letters **10**, 518 (1963); U. Fano and J. W. Cooper, Phys. Rev. **137**, A1364 (1965).

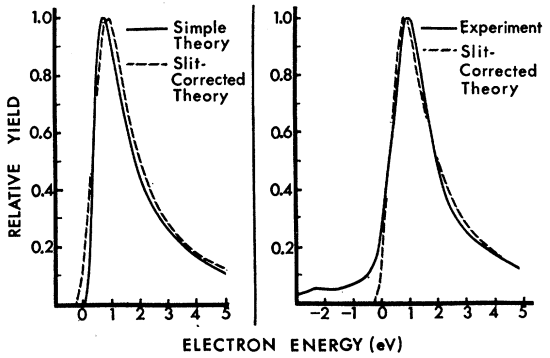

FIG. 5. A comparison of the shape of the auto-ionization peak as predicted by the ion field theory and as observed for 4-keV He^+ in He. The experimental value of the effective slit width was used to modify the calculated distribution to obtain the curve labeled "slit-corrected theory." The zero of the electron energy is the value expected for the auto-ionization transition in the isolated atom.

the electron spectrum is given by

$$\frac{1}{N_0}\frac{dN}{dE}=\frac{b}{P^2}\exp(-b/P),$$

where $(1/N_0)dN/dE$ is the energy distribution, P is the depression of the electron energy in eV from that at infinite nuclear separation, and $b=e/(4\pi\epsilon_0 v\tau)$. In this, v is the ion velocity at infinite separation, τ the mean lifetime of the auto-ionizing state, e the electronic charge, and ϵ_0 the permittivity of free space. In Fig. 5, this line shape is plotted first uncorrected for the apparatus slit width, corrected for this, and, finally, compared with the experimental distribution for 4-keV ions. The high-energy end of the experimental curve is distorted by the presence of the small additional auto-ionizing peak. Expressed in a dimensionless variable $z=b/P$, the peak maximum occurs at a value of z of $\frac{1}{2}$, and the width of the peak is 1.07. Thus one would expect the observed dependence of both the energy of the peak maximum and the width on the inverse square root of the ion energy.

For He^+ in He, the above gives the mean lifetime of the auto-ionizing state $He(2s2p)$ as

$$\tau=-(1.04\times10^{-13})(dV^{-1/2}/dE),$$

where V is the ion beam energy in keV and E is the auto-ionization peak energy in eV. The experimental results for the peak energy relative to the zero of self-energy yield $dV^{-1/2}/dE=-(0.026\pm0.007)$ in units of $(\text{eV})^{-3/2}$, and, therefore, a value of $\tau=(2.70\pm0.69)\times10^{-15}$ sec. This model gives from the variation of width at half-maximum a lifetime

$$\tau=(2.23\times10^{-13})dV^{-1/2}/dW,$$

where W is the peak width in eV. The experimentally determined dependence $dV^{-1/2}/dW=(1.05\pm0.08)\times10^{-2}$ $(\text{eV})^{-3/2}$ results in a $\tau=(2.36\pm0.17)\times10^{-15}$ sec. This value of τ was used in fitting the calculated line shape to the experimental 4-keV ion energy in Fig. 5.

The only other experimental value of the lifetime of the $He(2s2p)\ ^1P$ auto-ionizing state has been determined by Madden and Codling[2] from far ultraviolet absorption in He and is $(1.72\pm0.18)\times10^{-14}$ sec. Burke, McVicar, and Smith[5] have calculated a lifetime for this state of 1.6×10^{-14} sec. Very likely the difference of almost an order of magnitude between these values and the lifetime deduced from the line shape originates in the assumptions on the nature of the ion field at the auto-ionizing atom and on the effect of this field on the lifetime of the state. Of course, the lifetime so determined is not then that of the isolated atom. Even less valid is the application of this model to the case of Ne^+ in He. The lifetimes obtained for the auto-ionizing states corresponding to the 22- and the 27-eV peaks are respectively $(3.5\pm1.2)\times10^{-15}$ sec and $(3.4\pm1.0)\times10^{-15}$ sec.

The electron energy corresponding to an auto-ionization at infinite nuclear separation found here are compared in Tables I and II with values found in a number of other studies. Those marked "?" are uncertain in that no determination of the dependence on ion velocity was possible. The numbers in parentheses are the energies of the auto-ionizing states assuming the ion ground state as the final state of the transition.

SUMMARY

The energy distribution of electrons from ionizing collisions of He and Ne ions in He reported here have been observed under conditions in which the instrumental slit width has only a minor effect on the distributions. The spectra are characterized by a continuous distribution which decreases rapidly from the value at the zero of electron energy wlth broad peaks of several eV in width occurring in the range of 20–40 eV. As the ion energy goes to infinity, the energy of the peak maxima approach a limit which is the energy of electrons ejected from known auto-ionizing states of the isolated atom.

Evidence from the change in peak energy and in the width of the peak with the relative velocity of the colliding particles supports the view that the entire distribution arises from the auto-ionization of the temporary molecule formed in the collision. The spectra then may be represented as the superposition of a number of distributions each associated with one auto-ionizing state. Each of these terminates in a peak which represents the "crowding" into a short energy range of those decays of an auto-ionizing molecular state that occur for internuclear separations extending from several angstroms to infinity.

ACKNOWLEDGMENT

We should like to express our appreciation to L. Juhlin for his assistance with the computer programming.